Hindawi Publishing Corporation
EURASIP Journal on Wireless Communications and Networking
Volume 2007, Article ID 26760, 11 pages
doi:10.1155/2007/26760

Research Article

Throughput Analysis of Large Wireless Networks with Regular Topologies

Kezhu Hong and Yingbo Hua

Department of Electrical Engineering, University of California, Riverside, CA 92521, USA

Received 2 September 2006; Revised 12 December 2006; Accepted 23 February 2007

Recommended by Weihua Zhuang

The throughput of large wireless networks with regular topologies is analyzed under two medium-access control schemes: synchronous array method (SAM) and slotted ALOHA. The regular topologies considered are square, hexagon, and triangle. Both nonfading channels and Rayleigh fading channels are examined. Furthermore, both omnidirectional antennas and directional antennas are considered. Our analysis shows that the SAM leads to a much higher network throughput than the slotted ALOHA. The network throughput in this paper is measured in either bits-hops per second per Hertz per node or bits-meters per second per Hertz per node. The exact connection between the two measures is shown for each topology. With these two fundamental units, the network throughput shown in this paper can serve as a reliable benchmark for future works on network throughput of large networks.

1. INTRODUCTION

The maximum achievable throughput of a large wireless network has been a topic of great interest. A large wireless network can take many possible forms in practice, which include large sensor networks, large ad hoc networks, and large mesh networks. A large mesh network may consist of a large number of wireless transceivers located (or approximately located) on a regular grid. Such a mesh network may serve as a virtual backbone for other mobile wireless clients. Since all nodes in the mesh network share the same wireless medium, the maximum network spectral efficiency (i.e., the maximum achievable network throughput) is of paramount importance. This is particularly true if the network is operating under heavy loads.

Until the recent works [1, 2], most of the research activities on maximum achievable throughput (i.e., capacity) of large wireless networks focus on scaling laws, for example, [3–5]. A capacity scaling law typically yields an upper bound on the maximum achievable throughput of the network, and the bound is often quite loose especially when applied to a given network topology. As argued in [1, 2], an exact and achievable throughput of a large network with a given topology is also of practical and theoretical importance. The throughput of a large mesh network is such an example. However, the throughput of a large network critically depends on medium-access control scheme.

In [2], a medium-access control scheme called synchronous array method (SAM) is proposed, and the network throughput of the SAM is analyzed under the nonfading channel condition and the square network topology. The essence of the SAM is that all packet transmissions in the network are orthogonal in time and/or frequency and the distance between any two adjacent transceivers is optimized to maximize the network spectral efficiency. It is shown in [2] that the throughput of the SAM is about 2–4 times the throughput of a well-known random-access scheme called slotted ALOHA [6].

In this paper, we present a further analysis of the SAM. In this analysis, we consider not only the square topology, but also the hexagonal and triangular topologies. We also consider the Rayleigh fading channels. Both omnidirectional antennas and directional antennas are treated in the analysis.

By network throughput we imply the maximum per-node uniform throughput under full load. By full load we imply that whenever a node is scheduled to transmit a packet in a given direction, there is at least one such packet available at the node.

To evaluate the network throughput, we will use two fundamental units: bits-hops/s/Hz/node and bits-meters/s/Hz/

node. The unit bits-hops/s/Hz/node measures the number of bits each node can transmit to its neighboring node in a given direction per second per Hertz. The unit bits-meters/s/Hz/node measures the number of bits transported over one-meter distance in an arbitrary direction (between source and destination) from each node per second per Hertz. The connection between the two units depends on the network topology, which will be shown under each of the three topologies to be considered.

A throughput analysis of the slotted ALOHA is shown in [1] where the throughput is expressed in packets/s/node. Although commonly used, this unit is not as fundamental as bits-hops/s/Hz/node or bits-meters/s/Hz/node as the latter takes into account the spectral efficiency of each packet while the former does not. It will be seen that the spectral efficiency of each packet can also be used to maximize the network throughput. We believe that a network throughput in bits-hops/s/Hz/node or bits-meters/s/Hz/node can serve as a more reliable benchmark than a network throughput in packets/s/node.

Note that according to Shannon's theory, the maximal spectral efficiency, that is, bits/s/Hz, that a packet can carry has the expression $\log_2(1+\eta)$, where η is the signal-to-interference-and-noise-ratio (SINR) threshold. When the actual SINR is larger than η, the packet is not detectible. When the actual SINR is less than η, the packet is detectible provided that the coding is perfect and the packet length is sufficiently long. By packet detection threshold we will refer to η.

A good review of other existing works on throughput analysis of large networks with regular topologies is available in [1], which we will not repeat.

The rest of this paper is organized as follows. In Section 2, we analyze the network throughput under SAM and nonfading channels for each of the three topologies: square, hexagon, and triangle. Also shown is the connection between bits-hops/s/Hz/node and bits-meters/s/Hz/node for each topology. The average source-destination (end-to-end) delay for each topology is also presented. In Section 3, we show the network throughput under SAM and fading channels for all three topologies. In Section 4, we present the network throughput under slotted ALOHA and fading channels for all three topologies. (For convenience, slotted ALOHA will also be referred to as ALOHA. The network throughput under ALOHA and nonfading channels is discussed in [2] and will not be addressed in this paper.) A comparison between SAM and ALOHA is summarized in Section 5.

2. NETWORK THROUGHPUT UNDER SAM AND NONFADING CHANNELS

The synchronous array method (SAM) schedules packet transmissions synchronously between arrays of nodes as summarized next. The network is partitioned into interleaved subsets (arrays) of nodes. During each time slot, a subset of nodes with a predetermined spacing is scheduled to transmit its packets towards its neighboring subset of nodes. Depending on the spacing of each subset of nodes, it takes several time slots for each node in the network to transmit a packet to its neighbor in a given direction. Depending on the network topology and the desired destination of a packet, there are several directions to which the packet can be transmitted. For each direction, the above process is repeated. The time slots referred to above can be replaced by frequency slots without affecting the network spectral efficiency. More details of the SAM will be revealed as we analyze the network throughput for three regular topologies.

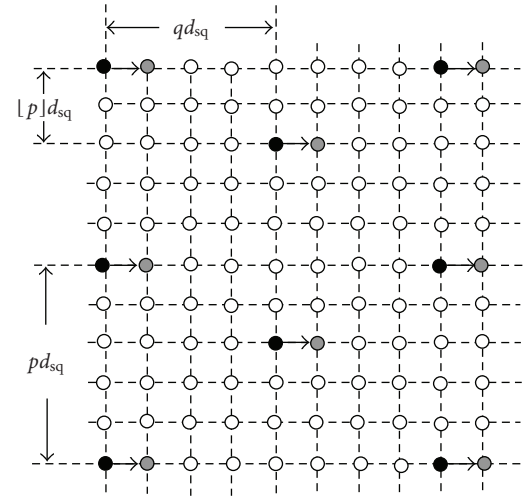

Figure 1: A network on the square grid with the spacing d_{sq} meters between two adjacent nodes. Under the SAM, data packets are transmitted from the black nodes to their neighboring gray nodes during a time slot. The vertical spacing between two active transceivers is pd_{sq} meters, and the horizontal spacing between two active transceivers is qd_{sq} meters. The offset between two adjacent columns of active transceivers is $\lfloor p/2 \rfloor d_{sq}$.

2.1. A network with square topology

Although partially presented in [2], this subsection is useful for completeness of this paper. A network on square grid is illustrated in Figure 1 where a subset of nodes is represented by the black nodes and its neighboring subset of nodes is represented by the gray nodes. During a time slot, the black nodes are the transmitting nodes, and the gray nodes are the receiving nodes. The sparseness (spacing) of the subset is determined by pd_{sq} and qd_{sq}, where p and q are integers and d_{sq} is the distance between two adjacent nodes. (The notation $\lfloor p \rfloor$ denotes the largest integer less than p.) Both the sparseness and the geometry of each subset affect the network throughput. The geometry shown in Figure 1 is expected to be ideal as the distance between any two pairs of transceivers is maximum for any given p and q.

For a different time slot, the location of the above-described two subsets of nodes is shifted left, right, up, or down. For every pq time slots, each of the nodes in the network has one chance to transmit a packet to its neighbor in a given direction. With the square topology, there are four possible directions for a packet to be transmitted from each node. The above process is repeated for each of the four directions.

To evaluate the network throughput, we first consider the signal-to-interference-and-noise ratio (SINR) at each receiving node during a time slot:

$$\text{SINR} = \frac{P_T/d_0^n}{\sigma^2 + \sum_{i\in S_{\text{sub}}} P_T/d_i^n} = \frac{1}{1/\text{SNR}_0 + \delta_{\text{SAM,sq}}}, \tag{1}$$

where $\text{SNR}_0 = P_T/\sigma^2 d_0^n$, P_T is the transmitted power from each transmitting node, σ^2 is the noise variance, d_0 is the distance between a receiver and its desired transmitter ($d_0 = d_{\text{sq}}$ for the square topology), d_i is the distance between the receiver and the ith interfering transmitters, n is the path loss exponent, and $\delta_{\text{SAM,sq}} = \sum_{i\in S_{\text{sub}}} d_0^n/d_i^n$ is referred to as the interference factor for the square grid, S_{sub} is the set of all interfering nodes.

In this paper, we consider a virtually infinite network. When the network is finite, the throughput shown in this paper is equivalent to a lower bound on the actual achievable throughput. The numerical results shown later are all based on the throughput of a center node in a network of about 200×200 nodes. The center node receives the largest interference, and hence governs a lower bound of the achievable (per node) network throughput.

If a directional antenna is used on each node, there is a power attenuation factor ξ between a receiver and a transmitter, which is defined as follows. $\xi = 1$ if the transmitter and the receiver are pointing to each other. $\xi = \epsilon$ ($\epsilon < 1$) if the transmitter is pointing to the receiver but the receiver is not pointing to the transmitter (or if the receiver is pointing to the transmitter but the transmitter is not pointing to the receiver). $\xi = \epsilon^2$ if none of the transmitter and the receiver is pointing to the other. In this case, the interference factor becomes $\delta_{\text{SAM,sq}} = \sum_i (d_0/d_i)^n \xi_i$, where ξ_i may be 1, ϵ, or ϵ^2 depending on the relative orientation of the interferer.

When P_T is sufficiently large, SINR becomes saturated at its upper bound $1/\delta_{\text{SAM,sq}}$. For the case of nonfading channels, we will only consider the saturated SINR and the corresponding network throughput.

We consider all interferences to be desired signals for other nodes. Since the best encoded waveform is Gaussian according to Shannon theory, it is reasonable to assume that the interferences are all Gaussian. Assuming that the noise and the interferences are all Gaussian and the network is (virtually) infinite, the network capacity in bits-hops/s/Hz/node is therefore

$$c_{\text{SAM,sq}} = \frac{1}{G_{\text{sq}}} \log_2\left(1 + \frac{1}{\delta_{\text{SAM,sq}}}\right), \tag{2}$$

where $G_{\text{sq}} = pq$ is the number of time slots needed for each of the nodes in the network to transmit once to its neighboring node in a given direction on the square grid. Note that $c_{\text{SAM,sq}}$ is an upper bound of the network capacity and is achievable when P_T is large. Here, each node is assumed to have a single antenna.

Based on the geometry of the subset of nodes as shown in Figure 1, one can verify that for $p > 1$,

$$\delta_{\text{SAM,sq}} = \delta_{\text{sq},1} + \delta_{\text{sq},2} + \delta_{\text{sq},3} + \delta_{\text{sq},4} + \delta_{\text{sq},5}, \tag{3}$$

Table 1: The (p, q)-optimal network throughput in bits-hops/s/Hz/node of a network on the square grid under the SAM and nonfading channels.

$c^*_{\text{SAM,sq}}, (p,q)^*$	$\epsilon = 1$	$\epsilon = 0.1$	$\epsilon = 0.01$
$n = 3$	0.2166, (2, 3)	1.7914, (1, 2)	2.1668, (1, 2)
$n = 4$	0.4208, (2, 3)	2.3780, (1, 2)	3.0442, (1, 2)
$n = 5$	0.6210, (2, 3)	2.7425, (1, 2)	3.8689, (1, 2)

where

$$\begin{aligned}
\delta_{\text{sq},1} &= \epsilon^2 \sum_{i=0}^{+\infty} \sum_{j=-\infty}^{+\infty} \sum_{g=0}^{1} \left(\left[(2i+1)q + (-1)^g\right]^2 + \left(pj - \left\lfloor \frac{p}{2} \right\rfloor\right)^2 \right)^{-n/2}, \\
\delta_{\text{sq},2} &= \epsilon^2 \sum_{i=0}^{+\infty} \sum_{j=-\infty}^{+\infty} \left(\left[2(i+1)q - 1\right]^2 + (pj)^2 \right)^{-n/2}, \\
\delta_{\text{sq},3} &= \epsilon^2 \sum_{i=0}^{+\infty} \sum_{j\neq 0} \left(\left[2(i+1)q + 1\right]^2 + (pj)^2 \right)^{-n/2}, \\
\delta_{\text{sq},4} &= \sum_{i=0}^{+\infty} \left(\left[2(i+1)q + 1\right]^2 \right)^{-n/2}, \\
\delta_{\text{sq},5} &= \epsilon^2 \sum_{j=1}^{+\infty} \left(1 + (pj)^2\right)^{-n/2}.
\end{aligned} \tag{4}$$

Referring to Figure 1, one can verify that $\delta_{\text{sq},1}$ corresponds to all the interferences from the transmitters located on the first column, third column, fifth column, and so on, to the left and right of each desired pair of transmitter and receiver; $\delta_{\text{sq},2}$ corresponds to all the interferences from the transmitters located on the second column, fourth column, and so on, to the right of each desired pair of transmitter and receiver; $\delta_{\text{sq},3}$ corresponds to all the interferences from the transmitters located on the second column, fourth column, and so on, to the left (except those in the line of sight) of each desired pair of transmitter and receiver; $\delta_{\text{sq},4}$ corresponds to all the interferences from the transmitters to the left and in the line of sight of each desired pair of transmitter and receiver; and $\delta_{\text{sq},5}$ is the interference from all the transmitters in the same column of each desired pair of transmitter and receiver.

For $p = 1$, one can similarly verify that

$$\begin{aligned}
\delta_{\text{SAM,sq}} = {} & \epsilon^2 \sum_{i=0}^{+\infty} \sum_{j=-\infty}^{+\infty} \left(\left[(i+1)q - 1\right]^2 + (pj)^2 \right)^{-n/2} \\
& + \epsilon^2 \sum_{i=0}^{+\infty} \sum_{j\neq 0} \left(\left[(i+1)q + 1\right]^2 + (pj)^2 \right)^{-n/2} \\
& + \sum_{i=0}^{+\infty} \left(\left[(i+1)q + 1\right]^2 \right)^{-n/2} + 2\epsilon^2 \sum_{j=1}^{+\infty} \left(1 + (pj)^2\right)^{-n/2}.
\end{aligned} \tag{5}$$

For each given pair of n and ϵ, the throughput $c_{\text{SAM,sq}}$ can be optimized over (p, q). Given in Table 1 are samples of the (p, q)-optimal $c_{\text{SAM,sq}}$ (denoted by $c^*_{\text{SAM,sq}}$) and the corresponding optimal (p, q) (denoted by $(p, q)^*$).

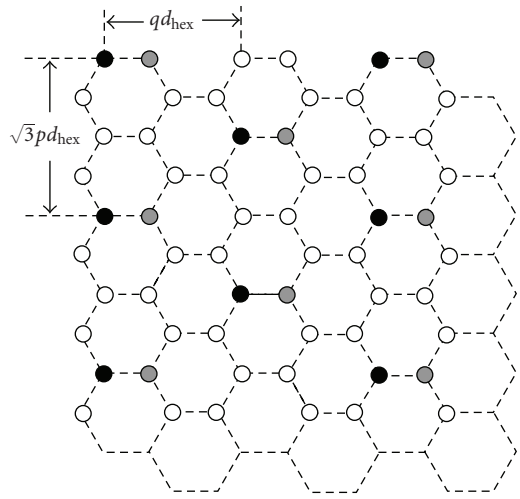

Figure 2: A network on the hexagonal grid with the spacing d_{hex} meters between two adjacent nodes. Under the SAM, data packets are transmitted from the black nodes to their neighboring gray nodes during a time slot. The horizontal spacing between two active transceivers is qd_{hex}, and the vertical spacing between two active transceivers is $\sqrt{3}pd_{\text{hex}}$.

Table 2: The (p, q)-optimal network throughput in bits-hops/s/Hz/node of a network on the hexagonal grid under the SAM and nonfading channels.

$c^*_{\text{SAM,hex}}, (p,q)^*$	$\epsilon = 1$	$\epsilon = 0.1$	$\epsilon = 0.01$
$n = 3$	0.2794, (1, 3)	2.1297, (1, 1.5)	2.7976, (1, 1.5)
$n = 4$	0.5430, (1, 3)	2.5813, (1, 1.5)	3.8645, (1, 1.5)
$n = 5$	0.8040, (1, 3)	2.7474, (1, 1.5)	4.8132, (1, 1.5)

2.2. A network with hexagonal topology

Following the same idea shown previously, we now consider a network on the hexagonal grid as illustrated in Figure 2 where a subset of transmission pairs during a time slot is denoted by the black and gray nodes. The vertical spacing between adjacent transmission pairs is denoted by $\sqrt{3}pd_{\text{hex}}$, and the horizontal spacing between adjacent transmission pairs is qd_{hex}. Here, p takes all natural integers. But q can be either $q = 3m$ or $q = 3m - 1.5$, where m is any natural integer.

With the hexagonal topology, each node has three possible directions for a packet transmission. In order for each node in the network to have one chance to transmit a packet to its neighbor in one of its three directions, we need $G_{\text{hex}} = 2p(2q/3)$ time slots if $q = 3m$ or $G_{\text{hex}} = 2p[2(q - 1.5)/3 + 1]$ time slots if $q = 3m - 1.5$. Then, the network throughput in bits-hops/s/Hz/node in one of three directions is given by

$$c_{\text{SAM,hex}} = \frac{1}{G_{\text{hex}}} \log_2 \left(1 + \frac{1}{\delta_{\text{SAM,hex}}}\right), \tag{6}$$

where $\delta_{\text{SAM,hex}}$ is the interference factor for the hexagonal topology. Following the geometry of the subset of nodes shown in Figure 2, one can verify that if $q = 3m$ and $p > 1$, then

$$\begin{aligned}\delta_{\text{SAM,hex}} = {} & \epsilon^2 \sum_{i=0}^{+\infty} \sum_{j=-\infty}^{+\infty} \sum_{g=0}^{1} \\ & \times \left(\left[(2i+1)q + (-1)^g\right]^2 + \left(\sqrt{3}pj - \left\lfloor \frac{p}{2} \right\rfloor \sqrt{3}\right)^2 \right)^{-n/2} \\ & + \epsilon^2 \sum_{i=0}^{+\infty} \sum_{j=-\infty}^{+\infty} \left(\left[2(i+1)q - 1\right]^2 + \left(\sqrt{3}pj\right)^2 \right)^{-n/2} \\ & + \epsilon^2 \sum_{i=0}^{+\infty} \sum_{j\neq 0} \left(\left[2(i+1)q + 1\right]^2 + \left(\sqrt{3}pj\right)^2 \right)^{-n/2} \\ & + \sum_{i=0}^{+\infty} \left(\left[2(i+1)q + 1\right]^2 \right)^{-n/2} \\ & + 2\epsilon^2 \sum_{j=1}^{+\infty} \left(1 + \left(\sqrt{3}pj\right)^2 \right)^{-n/2}\end{aligned} \tag{7}$$

and if $q = 3m$ and $p = 1$, then

$$\begin{aligned}\delta_{\text{SAM,hex}} = {} & \epsilon^2 \sum_{i=0}^{+\infty} \sum_{j=-\infty}^{+\infty} \left(\left[(i+1)q - 1\right]^2 + \left(\sqrt{3}pj\right)^2 \right)^{-n/2} \\ & + \epsilon^2 \sum_{i=0}^{+\infty} \sum_{j\neq 0} \left(\left[(i+1)q + 1\right]^2 + \left(\sqrt{3}pj\right)^2 \right)^{-n/2} \\ & + \sum_{i=0}^{+\infty} \left(\left[(i+1)q + 1\right]^2 \right)^{-n/2} \\ & + 2\epsilon^2 \sum_{j=1}^{+\infty} \left(1 + \left(\sqrt{3}pj\right)^2 \right)^{-n/2}.\end{aligned} \tag{8}$$

Furthermore, if $q = 3m - 1.5$, then

$$\begin{aligned}\delta_{\text{SAM,hex}} = {} & \epsilon^2 \sum_{i=0}^{+\infty} \sum_{j=-\infty}^{+\infty} \left(\left[(2i+1)q - 1\right]^2 + \left[\sqrt{3}pj - \left(\frac{1}{2} + \left\lfloor \frac{p}{2} \right\rfloor\right)\sqrt{3}\right]^2 \right)^{-n/2} \\ & + \epsilon^2 \sum_{i=0}^{+\infty} \sum_{j=-\infty}^{+\infty} \left(\left[(2i+1)q + 1\right]^2 + \left[\sqrt{3}pj - \left(\frac{1}{2} + \left\lfloor \frac{p}{2} \right\rfloor\right)\sqrt{3}\right]^2 \right)^{-n/2} \\ & + \epsilon^2 \sum_{i=0}^{+\infty} \sum_{j=-\infty}^{+\infty} \left(\left[2(i+1)q - 1\right]^2 + \left(\sqrt{3}pj\right)^2 \right)^{-n/2} \\ & + \epsilon^2 \sum_{i=0}^{+\infty} \sum_{j\neq 0} \left(\left[2(i+1)q + 1\right]^2 + \left(\sqrt{3}pj\right)^2 \right)^{-n/2} \\ & + \sum_{i=0}^{+\infty} \left(\left[2(i+1)q + 1\right]^2 \right)^{-n/2} + 2\epsilon^2 \sum_{j=1}^{+\infty} \left(1 + \left(\sqrt{3}pj\right)^2 \right)^{-n/2}.\end{aligned} \tag{9}$$

Shown in Table 2 are samples of the (p, q)-optimal $c_{\text{SAM,hex}}$ and the corresponding optimal (p, q).

2.3. A network with triangle topology

A network on the triangle grid is shown in Figure 3 where a subset of transmission pairs during a time slot is marked

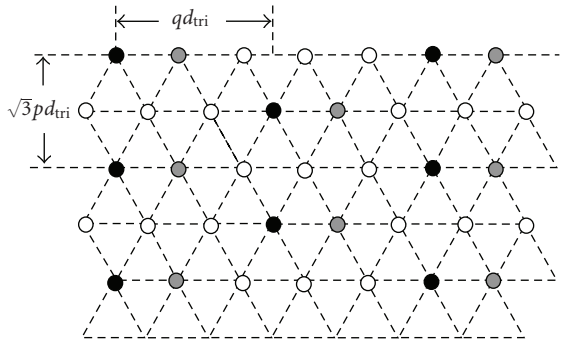

Figure 3: A network on the triangular grid with the spacing d_{tri} meters between two adjacent nodes. Under the SAM, data packets are transmitted from the black nodes to their neighboring gray nodes during a time slot. The horizontal spacing between two active transceivers is qd_{tri} and the vertical spacing between two active transceivers is $\sqrt{3}pd_{\text{tri}}$.

Table 3: The (p,q)-optimal throughput in bits-hops/s/Hz/node of a network on the triangular grid under the SAM and nonfading channels.

$c^*_{\text{SAM,tri}}, (p,q)^*$	$\epsilon = 1$	$\epsilon = 0.1$	$\epsilon = 0.01$
$n = 3$	0.1863, (1, 3)	1.4198, (1, 1.5)	1.8651, (1, 1.5)
$n = 4$	0.3620, (1, 3)	1.7209, (1, 1.5)	2.5763, (1, 1.5)
$n = 5$	0.5360, (1, 3)	1.8316, (1, 1.5)	3.2088, (1, 1.5)

by black and gray nodes. The vertical spacing of transmission pairs is $\sqrt{3}pd_{\text{tri}}$, and the horizontal spacing is qd_{tri}. Here, p takes any natural integers, but q can be either m or $m - 0.5$, where m is a natural integer. The number of time slots required for all nodes in the network to transmit once in one of six possible directions is $G_{\text{tri}} = 2pq$ if $q = m$, or $G_{\text{tri}} = p[2(q - 0.5) + 1]$ if $q = m - 0.5$. The capacity in bits-hops/s/Hz/node is therefore

$$c_{\text{SAM,tri}} = \frac{1}{G_{\text{tri}}} \log_2 \left(1 + \frac{1}{\delta_{\text{SAM,tri}}}\right), \tag{10}$$

where $\delta_{\text{SAM,tri}}$ is the interference factor for the triangular topology.

One can verify that if $q = 1, 2, 3\ldots$ and $p = 2, 3, 4\ldots$, then

$$\begin{aligned}
\delta_{\text{SAM,tri}} &= \epsilon^2 \sum_{i=0}^{+\infty} \sum_{j=-\infty}^{+\infty} \sum_{g=0}^{1} \left(\left[(2i+1)q + (-1)^g\right]^2 + \left(\sqrt{3}pj - \left\lfloor \frac{p}{2} \right\rfloor \sqrt{3}\right)^2 \right)^{-n/2} \\
&\quad + \epsilon^2 \sum_{i=0}^{+\infty} \sum_{j=-\infty}^{+\infty} \left(\left[2(i+1)q - 1\right]^2 + \left(\sqrt{3}pj\right)^2 \right)^{-n/2} \\
&\quad + \epsilon^2 \sum_{i=0}^{+\infty} \sum_{j\neq 0} \left(\left[2(i+1)q + 1\right]^2 + \left(\sqrt{3}pj\right)^2 \right)^{-n/2} \\
&\quad + \sum_{i=0}^{+\infty} \left(\left[2(i+1)q + 1\right]^2 \right)^{-n/2} + 2\epsilon^2 \sum_{j=1}^{+\infty} \left(1 + \left(\sqrt{3}pj\right)^2\right)^{-n/2}.
\end{aligned} \tag{11}$$

If $q = 1, 2, 3\ldots$ and $p = 1$, then

$$\begin{aligned}
\delta_{\text{SAM,tri}} &= \epsilon^2 \sum_{i=0}^{+\infty} \sum_{j=-\infty}^{+\infty} \left(\left[(i+1)q - 1\right]^2 + \left(\sqrt{3}pj\right)^2 \right)^{-n/2} \\
&\quad + \epsilon^2 \sum_{i=0}^{+\infty} \sum_{j\neq 0} \left(\left[(i+1)q + 1\right]^2 + \left(\sqrt{3}pj\right)^2 \right)^{-n/2} \\
&\quad + \sum_{i=0}^{+\infty} \left(\left[(i+1)q+1\right]^2 \right)^{-n/2} + 2\epsilon^2 \sum_{j=1}^{+\infty} \left(1 + \left(\sqrt{3}pj\right)^2\right)^{-n/2}.
\end{aligned} \tag{12}$$

If $q = 0.5, 1.5, 2.5\ldots$ and $p = 1, 2, 3\ldots$, then

$$\begin{aligned}
&\delta_{\text{SAM,tri}}(n) \\
&= \epsilon^2 \sum_{i=0}^{+\infty} \sum_{j=-\infty}^{+\infty} \left(\left[(2i+1)q - 1\right]^2 + \left[\sqrt{3}pj - \left(\frac{1}{2} + \left\lfloor \frac{p}{2} \right\rfloor\right)\sqrt{3}\right]^2 \right)^{-n/2} \\
&\quad + \epsilon^2 \sum_{i=0}^{+\infty} \sum_{j=-\infty}^{+\infty} \left(\left[(2i+1)q + 1\right]^2 + \left[\sqrt{3}pj - \left(\frac{1}{2} + \left\lfloor \frac{p}{2} \right\rfloor\right)\sqrt{3}\right]^2 \right)^{-n/2} \\
&\quad + \epsilon^2 \sum_{i=0}^{+\infty} \sum_{j=-\infty}^{+\infty} \left(\left[2(i+1)q - 1\right]^2 + \left(\sqrt{3}pj\right)^2 \right)^{-n/2} \\
&\quad + \epsilon^2 \sum_{i=0}^{+\infty} \sum_{j\neq 0} \left(\left[2(i+1)q + 1\right]^2 + \left(\sqrt{3}pj\right)^2 \right)^{-n/2} \\
&\quad + \sum_{i=0}^{+\infty} \left(\left[2(i+1)q + 1\right]^2 \right)^{-n/2} + 2\epsilon^2 \sum_{j=1}^{+\infty} \left(1 + \left(\sqrt{3}pj\right)^2\right)^{-n/2}.
\end{aligned} \tag{13}$$

We see that $\delta_{\text{SAM,tri}}(n)$ and $\delta_{\text{SAM,hex}}(n)$ have a similar structure. This is because if we add a node inside each hexagon of the network on the hexagonal grid, the network topology becomes triangular.

The (p,q)-optimal $c_{\text{SAM,tri}}$ and the corresponding optimal (p,q) are illustrated in Table 3.

2.4. Throughput comparison

In the previous subsections, we have evaluated the network throughput c in bits-hops/s/Hz/node for each of the three topologies. But in order to compare the throughput of different topologies fairly, we need to derive the network throughput α in bits-meters/s/Hz/node. Furthermore, we will fix the node density ρ for all topologies as well.

Let the smallest square area surrounded by four nodes in the square topology be denoted by A_{sq}, the smallest hexagonal area surrounded by six nodes in the hexagonal topology by A_{hex}, and the smallest triangular area defined by three nodes in the triangular topology by A_{tri}. Then, a simple analysis shows that for an infinite network, there is one node for every square on the square grid, 2 nodes for every hexagon on the hexagonal grid, and 0.5 node for every triangle on the triangular grid, that is,

$$\frac{1}{A_{\text{sq}}} = \rho, \qquad \frac{2}{A_{\text{hex}}} = \rho, \qquad \frac{0.5}{A_{\text{tri}}} = \rho. \tag{14}$$

Table 4: Comparison of the network throughput in bits-meters/s/Hz/node under $\rho = 1$.

$\alpha^*_{\text{SAM,sq}}, \alpha^*_{\text{SAM,hex}}, \alpha^*_{\text{SAM,tri}}$	$\epsilon = 1$			$\epsilon = 0.1$			$\epsilon = 0.01$		
$n = 3$	0.170	0.193	0.182	1.407	1.468	1.384	1.702	1.928	1.818
$n = 4$	0.331	0.374	0.353	1.868	1.779	1.677	2.391	2.663	2.511
$n = 5$	0.488	0.554	0.522	2.154	1.893	1.785	3.039	3.317	3.127

It is also easy to show that

$$A_{\text{sq}} = d_{\text{sq}}^2, \qquad A_{\text{hex}} = \frac{3\sqrt{3}}{2} d_{\text{hex}}^2, \qquad A_{\text{tri}} = \frac{\sqrt{3}}{4} d_{\text{tri}}^2. \tag{15}$$

Therefore,

$$d_{\text{sq}} = \sqrt{\frac{1}{\rho}}, \qquad d_{\text{hex}} = \sqrt{\frac{4}{3\sqrt{3}\rho}}, \qquad d_{\text{tri}} = \sqrt{\frac{2}{\sqrt{3}\rho}}. \tag{16}$$

On the square grid, the number of hops required for a packet to move over a long distance D (with $D \gg d_{\text{sq}}$) in an arbitrary direction $\theta \in [0, \pi/4]$ is given by

$$N_{\text{sq}} = \left| \frac{D\cos(\pi/4 - \theta)}{\sqrt{2} d_{\text{sq}}} \times 2 \right|. \tag{17}$$

Since the average number of hops in each of the $\pi/4$-angle partitions of the interval $0 \le \theta < 2\pi$ is the same, the average number of hops for any $\theta \in [0, 2\pi)$ is

$$\overline{N}_{\text{sq}} = \frac{4}{\pi} \int_0^{\pi/4} N_{\text{sq}} d\theta = \frac{4}{\pi} \frac{D}{d_{\text{sq}}}. \tag{18}$$

Similarly, we can show that for the hexagonal grid,

$$N_{\text{hex}} = \frac{D\cos\phi}{3 d_{\text{hex}}} \times 4, \quad \text{for } \phi \in \left[0, \frac{\pi}{6}\right], \tag{19}$$

and hence

$$\overline{N}_{\text{hex}} = \frac{6}{\pi} \int_0^{\pi/6} N_{\text{hex}} d\phi = \frac{4}{\pi} \frac{D}{d_{\text{hex}}}. \tag{20}$$

For the triangular grid, we have

$$N_{\text{tri}} = \frac{D\cos(\pi/6 - \varphi)}{\sqrt{3} d_{\text{tri}}} \times 2, \quad \text{for } \varphi \in \left[0, \frac{\pi}{6}\right], \tag{21}$$

and hence

$$\overline{N}_{\text{tri}} = \frac{6}{\pi} \int_0^{\pi/6} N_{\text{tri}} d\phi = \frac{6}{\sqrt{3}\pi} \frac{D}{d_{\text{tri}}}. \tag{22}$$

The throughput α in bits-meters/s/Hz/node is simply the throughput c in bits-hops/s/Hz/node multiplied by the average number of meters per hop, that is,

$$\begin{aligned}
\alpha_{\text{SAM,sq}} &= \frac{D}{\overline{N}_{\text{sq}}} c_{\text{SAM,sq}} \\
&= \frac{\pi}{4} c_{\text{SAM,sq}} \sqrt{\frac{1}{\rho}} \approx 0.785 c_{\text{SAM,sq}} \sqrt{\frac{1}{\rho}}, \\
\alpha_{\text{SAM,hex}} &= \frac{D}{\overline{N}_{\text{hex}}} c_{\text{SAM,hex}} \\
&= \frac{\pi}{4} \sqrt{\frac{4}{3\sqrt{3}}} c_{\text{SAM,hex}} \sqrt{\frac{1}{\rho}} \approx 0.689 c_{\text{SAM,hex}} \sqrt{\frac{1}{\rho}}, \\
\alpha_{\text{SAM,tri}} &= \frac{D}{\overline{N}_{\text{tri}}} c_{\text{SAM,tri}} \\
&= \frac{\sqrt{3}\pi}{6} \sqrt{\frac{2}{\sqrt{3}}} c_{\text{SAM,tri}} \sqrt{\frac{1}{\rho}} \approx 0.975 c_{\text{SAM,tri}} \sqrt{\frac{1}{\rho}}.
\end{aligned} \tag{23}$$

We see that the relationship between α and c is only weakly affected by the network topology.

Table 4 illustrates the (p, q)-optimized $\alpha_{\text{SAM,sq}}$, $\alpha_{\text{SAM,hex}}$, and $\alpha_{\text{SAM,tri}}$ under $\rho = 1$. We can see that $\alpha^*_{\text{SAM,hex}}$ is the largest when $\epsilon = 1$ or $\epsilon \ll 1$. When $\epsilon = 0.1$, $\alpha^*_{\text{SAM,sq}}$ becomes the largest for large n. Overall, the difference among $\alpha^*_{\text{SAM,sq}}$, $\alpha^*_{\text{SAM,hex}}$, and $\alpha^*_{\text{SAM,tri}}$ is not very large.

2.5. Delay analysis

The average source-to-destination or end-to-end delay T_{E2E} is also useful. We next evaluate T_{E2E} for each of the three topologies.

With the same node density ρ and the same source-destination distance D, the average delay T_{E2E} in a network can be expressed as

$$T_{\text{E2E}} = KG^*\overline{N}T, \tag{24}$$

where K denotes the number of possible transmission directions from each node, G^* the optimal number of time slots needed for each node to transmit a packet, $\overline{N}$ the average number of hops needed for a packet to travel D meters, and T is the duration of each time slot that is assumed to be the same for all topologies. The value of K is 4 for the square grid, 3 for the hexagonal grid, and 6 for the triangular grid. The value of G^* is determined by the optimal sparseness parameters, which can be easily computed based on the results in the previous subsections. The expressions of $\overline{N}$ for the three topologies are available in the previous subsection.

Table 5: Normalized T_{E2E} for networks on the square, hexagonal, and triangular grids.

E2E delay	$\epsilon = 1$	$\epsilon = 0.1, 0.01$
$T_{\text{E2E,sq}}$	96.00	32.00
$T_{\text{E2E,hex}}$	54.71	27.35
$T_{\text{E2E,tri}}$	116.05	58.03

One can verify that for the square grid,

$$T_{\text{E2E,sq}} = 16G^*_{\text{sq}}\left(\frac{D}{\pi}\right)\sqrt{\rho}T, \tag{25}$$

and for the hexagonal grid,

$$T_{\text{E2E,hex}} = 6\sqrt{3\sqrt{3}}G^*_{\text{hex}}\left(\frac{D}{\pi}\right)\sqrt{\rho}T \tag{26}$$

and for the triangular grid,

$$T_{\text{E2E,tri}} = 6\sqrt{6\sqrt{3}}G^*_{\text{tri}}\left(\frac{D}{\pi}\right)\sqrt{\rho}T. \tag{27}$$

Table 5 shows $T_{\text{E2E,sq}}$, $T_{\text{E2E,hex}}$, and $T_{\text{E2E,tri}}$ under $(D/\pi)\sqrt{\rho}T = 1$. From this table, we observe that $T_{\text{E2E,hex}}$ is the smallest for both omnidirectional and directional antennas, and $T_{\text{E2E,tri}}$ is the largest.

3. NETWORK THROUGHPUT UNDER SAM AND FADING CHANNELS

We now assume that all channels in the network are block Rayleigh fading channels. Then, the SINR at a receiving node is given by

$$\text{SINR} = \frac{r_0}{\sigma^2 + \sum_{i\in S_{\text{sub}}} r_i}, \tag{28}$$

where r_0 is the received power of the desired signal, r_i is the received power from the ith interferer, σ^2 is the noise power, and S_{sub} denotes the set of all interfering nodes in a subset of transmitting nodes under the SAM. With the Rayleigh fading model (on the amplitude of complex channel coefficients), the probability density function of r_i for any i is given by the exponential function

$$p_{r_i}(x) = \frac{1}{\overline{r}_i}\exp\left(-\frac{x}{\overline{r}_i}\right), \tag{29}$$

where $\overline{r}_i = P_T d_i^{-n}\xi_i$, and P_T, d_i, n, and ξ_i were defined before.

We also assume that each packet is encoded with the (ideal) spectral efficiency $R = \log_2(1+\eta)$ in bits/s/Hz, where η is the expected SINR. Then, similar to an analysis shown in [1], the probability for a packet to be successfully received is

$$\begin{aligned}
P_{\text{SAM}} &= \text{Prob}\{\text{SINR} \geq \eta\} \\
&= \text{Prob}\left\{r_0 \geq \eta\left(\sigma^2 + \sum_{i\in S_{\text{sub}}} r_i\right)\right\} \\
&= E_{\{r_i, i\in S_{\text{sub}}\}}\left\{\int_{\eta\sigma^2+\sum_{i\in S_{\text{sub}}} r_i}^{+\infty} \frac{1}{\overline{r}_0}\exp\left(-\frac{x}{\overline{r}_0}\right)dx\right\} \\
&= \exp\left(-\eta\frac{\sigma^2}{\overline{r}_0}\right)E_{\{r_i, i\in S_{\text{sub}}\}}\left\{\exp\left(-\eta\frac{\sum_{i\in S_{\text{sub}}} r_i}{\overline{r}_0}\right)\right\} \\
&= \exp\left(-\eta\frac{\sigma^2}{\overline{r}_0}\right)\prod_{i\in S_{\text{sub}}}\int_0^{+\infty}\exp\left(-\frac{\eta x}{\overline{r}_0}\right)p_{r_i}(x)dx \\
&= \exp\left(-\eta\frac{\sigma^2}{\overline{r}_0}\right)\prod_{i\in S_{\text{sub}}}\frac{\overline{r}_0}{\overline{r}_0 + \eta\overline{r}_i} \\
&= \exp\left(-\eta\frac{\sigma^2 d_0^n}{P_T}\right)\prod_{i\in S_{\text{sub}}}\frac{1}{1+\eta(d_0/d_i)^n\xi_i} \\
&\leq \prod_{i\in S_{\text{sub}}}\frac{1}{1+\eta(d_0/d_i)^n\xi_i},
\end{aligned} \tag{30}$$

where $E_{\{r_i, i\in S_{\text{sub}}\}}$ denotes expectation with respect to the set of random variables $\{r_i, i \in S_{\text{sub}}\}$, and the independence among $\{r_i, i \in S_{\text{sub}}\}$ is assumed. The last upper bound on P_{SAM} is achieved (approximately) as long as P_T is sufficiently large. Since d_i and ξ_i are topology-dependent, so is P_{SAM}.

The network throughput in bits-hops/s/Hz/node under the SAM and the Rayleigh fading channels is given by

$$c_{\text{SAM,fading}} = \frac{R}{G}P_{\text{SAM}}, \tag{31}$$

where G is the number of the time slots required for each node to have a chance to transmit a packet, which is a topology-dependent function of the sparseness parameters p and q as shown before. Like c_{SAM}, $c_{\text{SAM,fading}}$ can be maximized over p and q for any given η, n, and ϵ.

The network throughput $\alpha_{\text{SAM,fading}}$ in bits-meters/s/Hz/node for each topology can be obtained from the corresponding $c_{\text{SAM,fading}}$ from one of the conversion equations (23). For convenience, we will set $\rho = 1$ and $\text{SNR}_0 = P_T/\sigma^2 d_0^n = 30$ dB.

Figure 4 illustrates the optimized $\alpha_{\text{SAM,fading,sq}}$ for the square topology versus the detection threshold η.

Figure 5 illustrates the optimized $\alpha_{\text{SAM,fading,hex}}$ for the hexagonal topology versus the detection threshold η.

Figure 6 illustrates the optimized $\alpha_{\text{SAM,fading,tri}}$ for the triangular topology versus the detection threshold η.

We see that the patterns of the network throughput for the three topologies are similar. The network throughput increases as the path loss exponent n increases and/or the relative attenuation ϵ of the directional antennas decreases. For any given n and ϵ, there is an optimal choice of the detection threshold η. The optimal η is around 5 dB when $\epsilon = 1$. As ϵ decreases and/or n increases, the optimal η increases. The "nonsmoothness" appearance of some of the curves is due

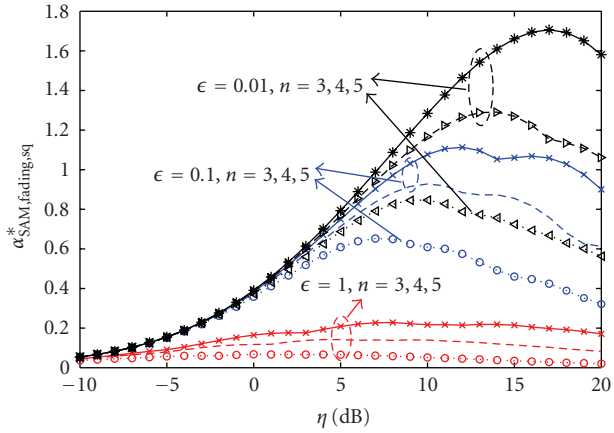

FIGURE 4: The (p, q)-optimized $\alpha_{\mathrm{SAM,fading,sq}}$ in bits-meters/s/Hz/node versus η for the square topology under $\mathrm{SNR}_0 = 30$ dB and $\rho = 1$.

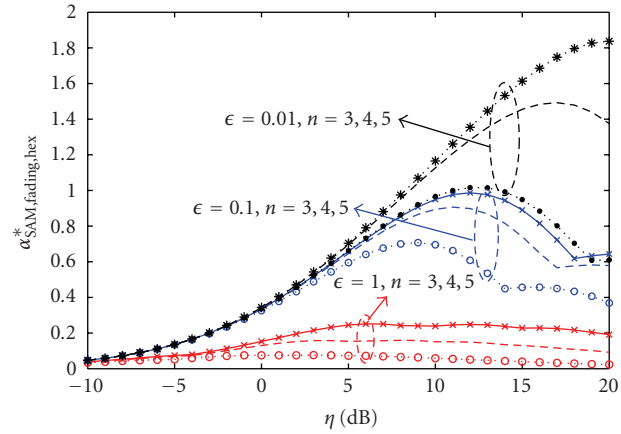

FIGURE 5: The (p, q)-optimized $\alpha_{\mathrm{SAM,fading,hex}}$ in bits-meters/s/Hz/node versus η for the hexagonal topology under $\mathrm{SNR}_0 = 30$ dB and $\rho = 1$.

to the change of optimal sparseness parameters p and q at different η. The optimal p and q (which are integers) "generally" increase as η (which is real) increases. Comparing the peak value of each of the curves in Figures 4, 5, and 6 with a corresponding value in Table 4, we see a loss of network throughput in the case of fading channels, which is expected.

Under the fading channels, a channel-aware opportunistic approach can be integrated into the SAM to improve the throughput, which is reported in [7]. We will not discuss this approach here. We next show an analysis of the slotted ALOHA under fading channels and compare its throughput with the results shown in this section. This comparison is important for one to appreciate the throughput difference between the SAM and the slotted ALOHA.

4. NETWORK THROUGHPUT UNDER ALOHA AND FADING CHANNELS

In this section, we evaluate the network throughput under (slotted) ALOHA and fading channels. For convenience, the slotted ALOHA is referred to as ALOHA.

A generic description of ALOHA is as follows. During each time slot, each node in the network transmits a packet with the probability p_t, or is ready to receive a packet with the probability $1 - p_t$.

However, to prepare for our analysis, more descriptions of ALOHA are needed. When a node becomes a transmitting node, it does not know which of its neighboring nodes is receiving. We assume that the transmitting node randomly picks a desired receiver (and hence a corresponding packet for that receiver). If the desired node is not in its receiving mode (and even if an unintended neighboring node receives the packet), the packet is deemed lost. In the case of omnidirectional antennas, a receiving node uses its received signal to decode each of all possible packets from its neighboring nodes. In the case of directional antennas, we assume that a receiving node uses (concurrently) four receiving antennas in the square topology, three receiving antennas in the

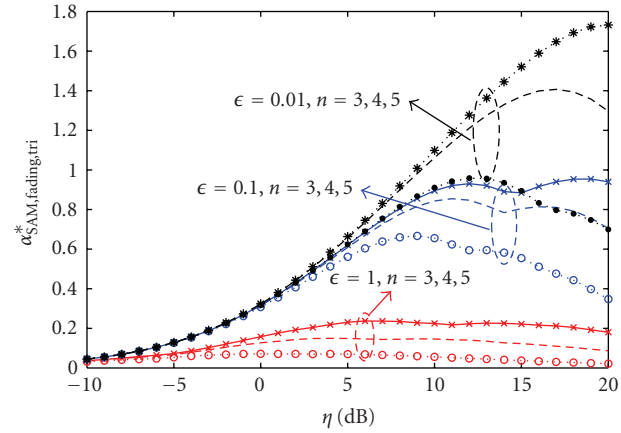

FIGURE 6: The (p, q)-optimized $\alpha_{\mathrm{SAM,fading,tri}}$ in bits-meters/s/Hz/node versus η for the triangular topology under $\mathrm{SNR}_0 = 30$ dB and $\rho = 1$.

hexagonal topology, or six receiving antennas in the triangular topology. All antennas on each node are pointing to different directions, and the signal received by each antenna is processed independently. A packet transmitted from a node is always transmitted from a correct directional antenna. A packet is deemed lost unless the transmitting antenna and its desired receiving antenna are pointing to each other. If we do not assume multiple receiving antennas for a receiving node, the network throughput of ALOHA is reduced by a factor (four, three, or six) depending on the topology.

Note that we ignore the idle state as it would only reduce the network throughput. Also, we do not consider incremental encoding and decoding although it could improve packet detection using data streams from different time slots. In this case, retransmissions of a previous failed packet are automatically taken into account in our analysis of network throughput.

We can now start the throughput analysis with the square topology. In this topology, each packet from a transmitter is meant for one of four possible directions (or receivers), and each receiver has four possible neighboring transmitters. Let P_{ALOHA} be the probability that a node receives a packet from a specific neighbor given that these two nodes are a desired transceiver pair. The probability that a node becomes a receiver and one specific neighbor becomes a transmitter and transmits a packet to the receiver is $(1/4)(1-p_t)p_t$. Considering that there are four neighbors for each receiving node, the probability that an arbitrary node receives a packet from (any or all of) its neighbors is therefore $(1-p_t)p_tP_{\text{ALOHA}}$. This simple expression holds for both omnidirectional antennas and directional antennas.

With a similar analysis, one can verify that for the hexagonal and triangular topologies, the probability that an arbitrary node receives a packet from (any or all of) its neighbors is still given by the same expression $(1-p_t)p_tP_{\text{ALOHA}}$.

If each packet carries $R = \log_2(1+\eta)$ bits/s/Hz, then the network throughput in bits-hops/s/Hz/node is

$$c_{\text{ALOHA,fading}} = (1-p_t)\,p_tP_{\text{ALOHA}}R, \tag{32}$$

and the network throughput in bits/meters/s/Hz/node is

$$\alpha_{\text{ALOHA,fading}} = (1-p_t)\,p_tP_{\text{ALOHA}}R\frac{D}{\overline{N}}, \tag{33}$$

where $D/\overline{N}$ is the average number of meters per hop, which depends on the topology as shown before.

Although the above expressions are simple, the details of P_{ALOHA} are tedious (especially for directional antennas) and dependent on the network topology. Next, we show how P_{ALOHA} can be derived.

Let us now assume that the node 0 and the node 1 are two neighboring nodes, the node 0 is receiving from the node 1, and the node 1 is transmitting to the node 0. Then the SINR at the receiving node is given by

$$\text{SINR} = \frac{r_0}{\sigma^2 + \sum_{i\neq 0,1}\xi_i s_i r_i}, \tag{34}$$

where s_i is a binary random variable with $\text{Prob}\{s_i = 1\} = p_t$ and $\text{Prob}\{s_i = 0\} = 1-p_t$, and ξ_i is a random power attenuation factor associated with directional antennas. As defined before, $\xi_i = 1$ if the receiving antenna at node 0 and the transmitting antenna at (interfering) node i are pointing to each other, $\xi_i = \epsilon$ if the receiving antenna at node 0 is pointing to node i who is however pointing away from node 0 or if node 0 is pointing away from node i who is pointing to node 0, and $\xi_i = \epsilon^2$ if both node 0 and node i are pointing away from each other. Since a transmitting node with directional antennas randomly picks a transmitting antenna, ξ_i is random. The probability distribution of ξ_i depends on the topology and the location of node i relative to the desired transceiver pair (i.e., node 0 and node 1).

Similar to (30), one can verify that for the square topology,

$$\begin{aligned}
P_{\text{ALOHA}} &= \text{Prob}\{\text{SINR} \geq \eta\} \\
&= \text{Prob}\left\{r_0 \geq \eta\left(\sigma^2 + \sum_{i\neq 0,1}\xi_i s_i r_i\right)\right\} \\
&= E_{\{\xi_i,\, i\neq 0,1\}}E_{\{s_i,\, i\neq 0,1\}}E_{\{r_i,\, i\neq 0,1\}} \\
&\quad\times\left\{\int_{\eta(\sigma^2+\sum_{i=0,1}\xi_i s_i r_i)}^{+\infty}\frac{1}{\overline{r}_0}\exp\left(-\frac{x}{\overline{r}_0}\right)dx\right\} \\
&= E_{\{\xi_i,\, i\neq 0,1\}}E_{\{s_i,\, i\neq 0,1\}}\exp\left(-\eta\frac{\sigma^2 d_0^n}{P_T}\right) \\
&\quad\times\prod_{i\neq 0,1}\frac{1}{1+\eta\xi_i s_i (d_0/d_i)^n} \\
&= \exp\left(-\eta\frac{\sigma^2 d_0^n}{P_T}\right) \\
&\quad\times\prod_{i\neq 0,1}\left(1-p_t+\sum_{j=1}^{4}\frac{p_t/4}{1+\eta\epsilon^{x_{\text{sq}}(i,j)}(d_0/d_i)^n}\right),
\end{aligned} \tag{35}$$

where $x_{\text{sq}}(i,j)$ takes a value from $\{0,1,2\}$, which depends on the location of node i and the orientation of the transmitting antenna at node i.

For the other two topologies, similar expressions of P_{ALOHA} follow from simple modifications in the last term of (35). More specifically, for the hexagonal topology, the sum in the last expression of (35) should be replaced by $\sum_{j=1}^{3}((p_t/3)/(1+\eta\epsilon^{x_{\text{hex}}(i,j)}(d_0/d_i)^n))$, where $x_{\text{hex}}(i,j)$ takes a value from $\{0,1,2\}$. And for the triangular topology, the sum in the last expression of (35) should be replaced by $\sum_{j=1}^{6}((p_t/6)/(1+\eta\epsilon^{x_{\text{tri}}(i,j)}(d_0/d_i)^n))$, where $x_{\text{tri}}(i,j)$ takes a value from $\{0,1,2\}$.

The exact choices of $x_{\text{sq}}(i,j)$, $x_{\text{hex}}(i,j)$, and $x_{\text{tri}}(i,j)$ are somewhat tedious but have been written into a computer program which we omit from this paper.

The network throughput $\alpha_{\text{ALOHA,fading}}$ depends on the transmission probability p_t of each node and the detection threshold η governed by the packet spectral efficiency R. For each value of η, $\alpha_{\text{ALOHA,fading}}$ can be maximized over p_t.

Figure 7 shows the p_t-optimal $\alpha_{\text{ALOHA,fading,sq}}$ versus η for different choices of ϵ and n for the square topology.

Figure 8 shows the p_t-optimal $\alpha_{\text{ALOHA,fading,hex}}$ versus η for different choices of ϵ and n for the hexagonal topology.

Figure 9 shows the p_t-optimal $\alpha_{\text{ALOHA,fading,tri}}$ versus η for different choices of ϵ and n for the triangular topology.

The p_t-optimal $\alpha_{\text{ALOHA,fading}}$ can be further optimized over η. The pattern of p_t-optimal $\alpha_{\text{ALOHA,fading}}$ versus η is similar to that of (p,q)-optimal $\alpha_{\text{SAM,fading}}$ versus η.

5. COMPARISON OF SAM AND ALOHA

Both the SAM and the (slotted) ALOHA require a time-slot synchronization, which is considered appropriate with modern electronic technology. Beyond that, the SAM requires all nodes in the network to know their relative positions so that the subsets of nodes can be scheduled properly.

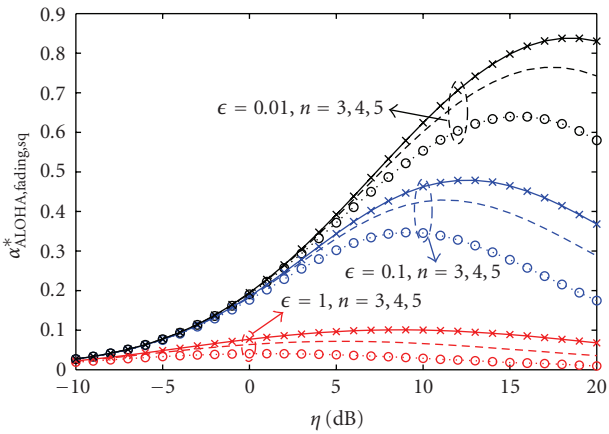

FIGURE 7: The p_t-optimal $\alpha_{\text{ALOHA,fading,sq}}$ in bits-meters/s/Hz/node versus η for the square topology under $\text{SNR}_0 = 30$ dB and $\rho = 1$.

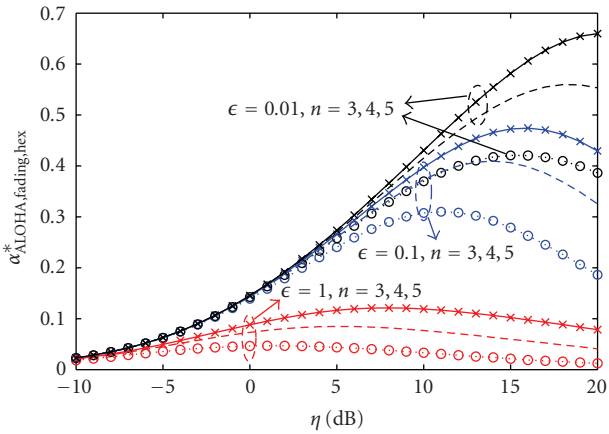

FIGURE 8: The p_t-optimal $\alpha_{\text{ALOHA,fading,hex}}$ in bits-meters/s/Hz/node versus η for the hexagonal topology under $\text{SNR}_0 = 30$ dB and $\rho = 1$.

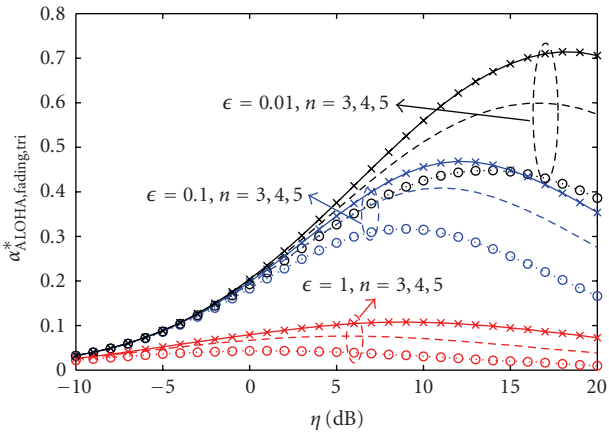

FIGURE 9: The p_t-optimal $\alpha_{\text{ALOHA,fading,tri}}$ in bits-meters/s/Hz/node versus η for the triangular topology under $\text{SNR}_0 = 30$ dB and $\rho = 1$.

The exact network topology is not necessary for the SAM as long as the actual topology can be approximately mapped to one of the regular topologies. Although the ALOHA does not need to know the topology since each node transmits a packet independently from other nodes, there is a significant routing overhead if the network topology is unknown to the nodes. For applications such as mesh networks, the nodes are relatively stationary and the network topology can be discovered in the initial stage of network setup. Once the network topology is known to all the nodes in the network, routing of packets is relatively easy. That is, when a packet needs to be transmitted from a node, the node first decides on the next-hop (neighboring) node based on the destination of the packet. This type of information is "stamped" on all packets to be transmitted from any node so that the node that receives a packet can identify whether or not the packet is intended for it. After a packet arrives at an intermediate (relay) node, a new stamp of the next hop replaces the old, and hence the packet size remains the same regardless of the source-destination distance of the packet. The throughput analysis of both the SAM and the ALOHA shown in this paper has been based on the above assumption.

Figure 10 compares the (p, q)-optimal $\alpha_{\text{SAM,fading}}$ versus η and the p_t-optimal $\alpha_{\text{ALOHA,fading}}$ versus η for each of the three topologies under $\epsilon = 1$ (omnidirectional antennas) and $\epsilon = 0.01$ (directional antennas), respectively. We see that when η is optimally chosen, the throughput of the SAM is about 2 to 3 times the throughput of the ALOHA.

6. CONCLUSIONS

In this paper, we have analyzed the throughput of large wireless networks with three regular topologies (square, hexagonal, and triangular). Two medium-access control schemes have been considered: synchronous array method (SAM) and a random-access method called slotted ALOHA. We have found that the three topologies do not change the network throughput significantly although the hexagonal topology has the smallest delay and the triangular topology has the largest delay. Our comparison between SAM and slotted ALOHA for fading channels shows that the SAM has a significantly higher throughput than slotted ALOHA. This finding is similar to a previous comparison between SAM and slotted ALOHA for nonfading channels.

Future work should consider protocols such as carrier-sense multiple access with collision avoidance (CSMA/CA). This protocol has been analyzed for small-size networks [8]. It should be useful to evaluate its performance in the context of large networks. Using fundamental throughput units such as bits-hops/s/Hertz/node should allow a fair comparison with SAM, ALOHA, as well as other schemes.

It is also useful to mention that directional antennas have been addressed by MAC researchers in recent years, for example, see [9]. But the work shown in this paper and [2] appears the first to provide a precise measure of the throughput gain using directional antennas.

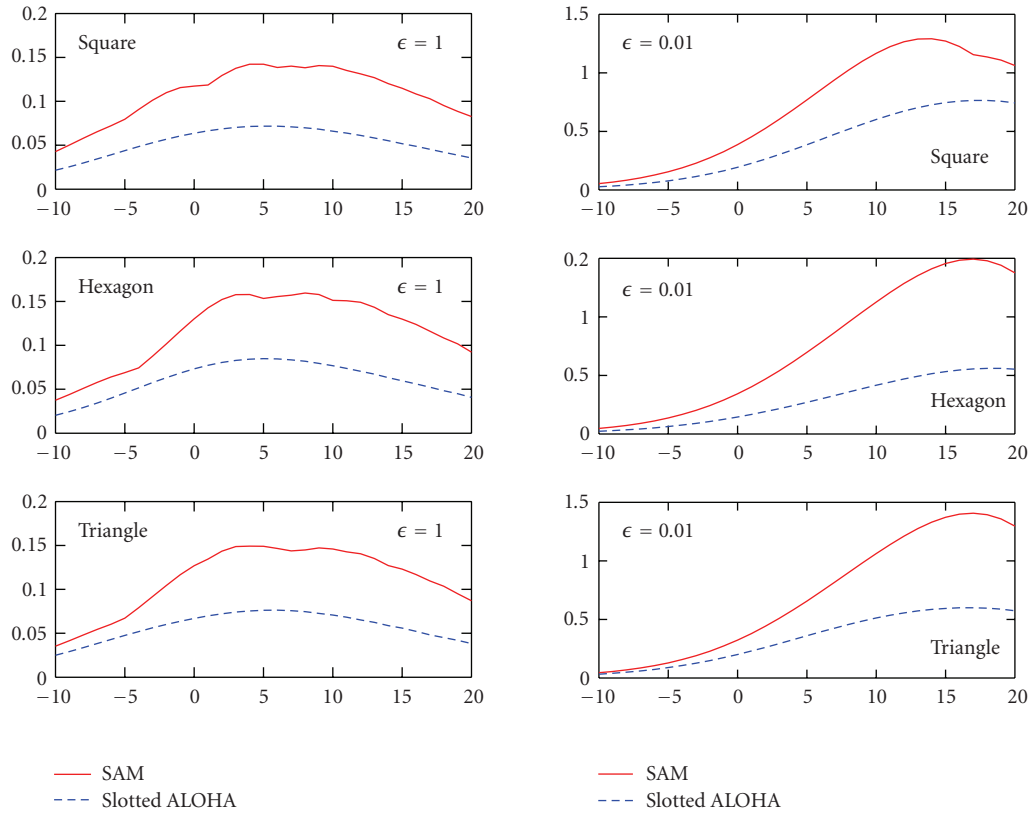

FIGURE 10: The (p, q)-optimal $\alpha_{\text{SAM,fading}}$ versus η in dB and the p_t-optimal $\alpha_{\text{ALOHA,fading}}$ versus η in dB for three topologies, $n = 4$, and $\text{SNR}_0 = 30\,\text{dB}$. The left column of plots is for $\epsilon = 1$ (omnidirectional antennas). The right column of plots is for $\epsilon = 0.01$ (directional antennas).

ACKNOWLEDGMENTS

This work was supported in part by the US National Science Foundation under Grant no. TF-0514736, and the US Army Research Office under the MURI Grant no. W911NF-04-1-0224. Part of this work was presented at IEEE Workshop on Sensor Array and Multichannel Processing, Waltham, Mass, July 2006.

REFERENCES

[1] X. Liu and M. Haenggi, "Throughput analysis of fading sensor networks with regular and random topologies," *EURASIP Journal on Wireless Communications and Networking*, vol. 2005, no. 4, pp. 554–564, 2005.

[2] Y. Hua, Y. Huang, and J. J. Garcia-Luna-Aceves, "Maximizing the throughput of large ad hoc wireless networks," *IEEE Signal Processing Magazine*, vol. 23, no. 5, pp. 84–94, 2006.

[3] L.-L. Xie and P. R. Kumar, "A network information theory for wireless communication: scaling laws and optimal operation," *IEEE Transactions on Information Theory*, vol. 50, no. 5, pp. 748–767, 2004.

[4] F. Xue, L.-L. Xie, and P. R. Kumar, "The transport capacity of wireless networks over fading channels," *IEEE Transactions on Information Theory*, vol. 51, no. 3, pp. 834–847, 2005.

[5] S. Yi, Y. Pei, and S. Kalyanaraman, "On the capacity improvement of ad hoc wireless networks using directional antennas," in *Proceedings of the the 4th ACM International Symposium on Mobile Ad Hoc Networking and Computing (MobiHoc '03)*, pp. 108–116, Annapolis, Md, USA, June 2003.

[6] *IEEE Transactions on Information Theory*, vol. 31, no. 2, 1985, special issue on Random-Access Communications.

[7] B. Zhao and Y. Hua, "A distributed medium access control scheme for a large network of wireless routers," submitted to *IEEE Transactions on Wireless Communications*.

[8] G. Bianchi, "Performance analysis of the IEEE 802.11 distributed coordination function," *IEEE Journal on Selected Areas in Communications*, vol. 18, no. 3, pp. 535–547, 2000.

[9] T. Korakis, G. Jakllari, and L. Tassiulas, "A MAC protocol for full exploitation of directional antennas in ad-hoc wireless networks," in *Proceedings of the the 4th ACM International Symposium on Mobile Ad Hoc Networking and Computing (MobiHoc '03)*, pp. 98–107, Annapolis, Md, USA, June 2003.